NE membrane (Fig. 3, D and E). The cytoplasm contains filaments of the cell's cytoskeleton, distinguishable according to size and morphology: actin fibers with a helical pitch, smooth intermediate filaments of variable diameters, and 13-protofilament microtubules (Fig. 3E and fig. S10). Occasionally, actin filaments formed direct physical connections to NPCs (Fig. 3E). With the NPCs embedded within the stiff lamina on one side and directly connected to the cytoskeleton on the other, it becomes feasible to comprehend how NPC diameter may differ considerably upon the action of mechanical forces.

In conclusion, the volumes reconstructed from these data reveal that many macromolecular complexes can be visually recognized without the need for computational averaging approaches and provide insight into structural variations at the level of individual complexes. Assisted by the synergistic application of recent technical developments, cryo-ET holds promise for revealing the molecular organization giving rise to cellular function in unperturbed environments.

REFERENCES AND NOTES

1. C. V. Robinson, A. Sali, W. Baumeister, *Nature* **450**, 973–982 (2007).
2. S. Pfeffer et al., *Nat. Commun.* **6**, 8403 (2015).
3. F. K. Schur et al., *Nature* **517**, 505–508 (2015).
4. M. Marko, C. Hsieh, R. Schalek, J. Frank, C. Mannella, *Nat. Methods* **4**, 215–217 (2007).
5. A. Rigort et al., *J. Struct. Biol.* **172**, 169–179 (2010).
6. C. Hsieh, T. Schmelzer, G. Kishchenko, T. Wagenknecht, M. Marko, *J. Struct. Biol.* **185**, 32–41 (2014).
7. J. Mahamid et al., *J. Struct. Biol.* **192**, 262–269 (2015).
8. R. Danev, S. Kanamaru, M. Marko, K. Nagayama, *J. Struct. Biol.* **171**, 174–181 (2010).
9. Y. Fukuda, U. Laugks, V. Lučić, W. Baumeister, R. Danev, *J. Struct. Biol.* **190**, 143–154 (2015).
10. P. Walther, Y. Chen, L. L. Pech, J. B. Pawley, *J. Microsc.* **168**, 169–180 (1992).
11. G. McMullan, A. R. Faruqi, D. Clare, R. Henderson, *Ultramicroscopy* **147**, 156–163 (2014).
12. S. Asano et al., *Science* **347**, 439–442 (2015).
13. R. Danev, B. Buijsse, M. Khoshouei, J. M. Plitzko, W. Baumeister, *Proc. Natl. Acad. Sci. U.S.A.* **111**, 15635–15640 (2014).
14. Materials and methods and supplementary text are available as supplementary materials on *Science* Online.
15. S. Pfeffer et al., *Nat. Commun.* **5**, 3072 (2014).
16. S. Pfeffer et al., *Structure* **20**, 1508–1518 (2012).
17. K. H. Bui et al., *Cell* **155**, 1233–1243 (2013).
18. T. Maimon, N. Elad, I. Dahan, O. Medalia, *Structure* **20**, 998–1006 (2012).
19. A. von Appen et al., *Nature* **526**, 140–143 (2015).
20. U. Aebi, J. Cohn, L. Buhle, L. Gerace, *Nature* **323**, 560–564 (1986).
21. C. W. Akey, *J. Cell Biol.* **109**, 955–970 (1989).
22. E. Grossman et al., *J. Struct. Biol.* **177**, 113–118 (2012).
23. K. Ben-Harush et al., *J. Mol. Biol.* **386**, 1392–1402 (2009).
24. D. S. Fudge, K. H. Gardner, V. T. Forsyth, C. Riekel, J. M. Gosline, *Biophys. J.* **85**, 2015–2027 (2003).
25. N. Mücke et al., *J. Mol. Biol.* **335**, 1241–1250 (2004).
26. J. Schäpe, S. Prausse, M. Radmacher, R. Stick, *Biophys. J.* **96**, 4319–4325 (2009).
27. K. Luger, A. W. Mäder, R. K. Richmond, D. F. Sargent, T. J. Richmond, *Nature* **389**, 251–260 (1997).
28. C. L. Woodcock, L. L. Frado, J. B. Rattner, *J. Cell Biol.* **99**, 42–52 (1984).
29. A. S. Frangakis et al., *Proc. Natl. Acad. Sci. U.S.A.* **99**, 14153–14158 (2002).

FOREST ECOLOGY

Leaf development and demography explain photosynthetic seasonality in Amazon evergreen forests

Jin Wu,[1]* Loren P. Albert,[1] Aline P. Lopes,[2] Natalia Restrepo-Coupe,[1,3] Matthew Hayek,[4] Kenia T. Wiedemann,[1,4] Kaiyu Guan,[5,6] Scott C. Stark,[7] Bradley Christoffersen,[1,8] Neill Prohaska,[1] Julia V. Tavares,[2] Suelen Marostica,[2] Hideki Kobayashi,[9] Mauricio L. Ferreira,[10,11] Kleber Silva Campos,[12] Rodrigo da Silva,[12] Paulo M. Brando,[13,14] Dennis G. Dye,[15] Travis E. Huxman,[16] Alfredo R. Huete,[3] Bruce W. Nelson,[2] Scott R. Saleska[1]*

In evergreen tropical forests, the extent, magnitude, and controls on photosynthetic seasonality are poorly resolved and inadequately represented in Earth system models. Combining camera observations with ecosystem carbon dioxide fluxes at forests across rainfall gradients in Amazônia, we show that aggregate canopy phenology, not seasonality of climate drivers, is the primary cause of photosynthetic seasonality in these forests. Specifically, synchronization of new leaf growth with dry season litterfall shifts canopy composition toward younger, more light-use efficient leaves, explaining large seasonal increases (~27%) in ecosystem photosynthesis. Coordinated leaf development and demography thus reconcile seemingly disparate observations at different scales and indicate that accounting for leaf-level phenology is critical for accurately simulating ecosystem-scale responses to climate change.

The seasonal rhythm of ecosystem metabolism—the aggregated photosynthesis, transpiration, or respiration of all organisms in a landscape—emerges from interactions among climate, ecology of individuals and communities, and biosphere-atmosphere exchange (*1*). In temperate zones, seasonality of terrestrial production drives annual oscillations in atmospheric carbon dioxide (*2*). In the tropics, plant transpiration seasonality mediates tropical convection and the timing of dry-to-wet season transitions—a potentially important climate feedback (*3*).

Seasonality in temperate zones is tightly linked to plant phenology (*4*) (the timing of periodic life-cycle events, including leaf development and senescence), which in turn is synchronized by cold-season dormancy (*4*). However, the extent, magnitude, and controls on seasonality of ecosystem metabolism in year-round warm tropical evergreen forest systems are less clear (*5–7*). For example, most current Earth system models represent little or no phenology in evergreen tropical biomes, so any seasonality in photosynthetic flux that emerges is due to seasonality in climatic drivers (*8–10*). However, remote-sensing observations (*5–7, 11–13*) suggest that central Amazon forests seasonally increase their photosynthetic capacity ("green-up") during dry seasons, whereas southern Amazon and African tropical forests show declines (*13*). There is extensive debate over the mechanisms driving these patterns (including whether they might be remote-sensing artifacts) (*5–7*) and how they might be modeled (*8–10, 14*).

To determine the extent of seasonality in tropical ecosystem photosynthesis (or gross ecosystem productivity, GEP), and to develop a more mechanistic understanding of how it emerges from climatic and biological processes, we address two key questions: (i) What is the relative importance of climatic drivers versus plant phenology in controlling GEP seasonality? (ii) What are the mechanisms by which these factors exert control? These questions conceptualize GEP as potentially driven by climate variability (e.g., temperature, light, or water) interacting with fixed photosynthetic infrastructure (e.g., leaf surface area, leaf photosynthetic capacity), or alternatively, by variability in that photosynthetic infrastructure, or some combination of the two.

To evaluate the first question, we compared GEP seasonality (derived from eddy covariance

measurements of ecosystem CO_2 exchange) to candidate explanatory variables at four Amazon sites distributed across gradients in rainfall and taxonomic composition. These variables include (i) five key climatic variables (*15*) and (ii) a metric of aggregate forest canopy phenology. The phenology metric—ecosystem-scale photosynthetic capacity (PC)—is an estimate of photosynthetic infrastructure independent of environment, derived

[1]Department of Ecology and Evolutionary Biology, University of Arizona, Tucson, AZ 85721, USA. [2]Brazil's National Institute for Amazon Research (INPA), Manaus, Amazonas, Brazil. [3]Plant Functional Biology and Climate Change Cluster, University of Technology Sydney, Sydney, NSW, Australia. [4]John A. Paulson School of Engineering and Applied Sciences, Harvard University, Cambridge, MA 02138, USA. [5]Department of Natural Resources and Environmental Science, University of Illinois at Urbana Champaign, Urbana, IL 61081, USA. [6]Department of Earth System Science, Stanford University, Stanford, CA 94025, USA. [7]Department of Forestry, Michigan State University, East Lansing, MI 48824, USA. [8]Earth and Environmental Sciences Division, Los Alamos National Lab, Los Alamos, NM 87545, USA. [9]Department of Environmental Geochemical Cycle Research, Japan Agency for Marine-Earth Science and Technology, Yokohama, Japan. [10]Centro de Energia Nuclear na Agricultura, University of Sao Paulo, Piracicaba, SP, Brazil. [11]Smart and Intelligent Cities Programme, University Nove de Julho, São Paulo, SP, Brazil. [12]Department of Environmental Physics, University of Western Para (UFOPA), Santarem, Para, Brazil. [13]Instituto de Pesquisa Ambiental da Amazônia (IPAM), Belem, Para, Brazil. [14]Woods Hole Research Center, Falmouth, MA 02450, USA. [15]Western Geographic Science Center, U.S. Geological Survey, Flagstaff, AZ 86001, USA. [16]Ecology and Evolutionary Biology and Center for Environmental Biology, University of California, Irvine, CA 92629, USA.
*Corresponding author. E-mail: jinwu@email.arizona.edu (J.W.); saleska@email.arizona.edu (S.R.S.)

by averaging the amount of photosynthesis per unit of incoming light, under fixed reference climatic conditions (*15*).

We found that GEP was strongly seasonal at all sites, but was not consistently driven by climate variability (Fig. 1 and table S4). Instead, GEP consistently tracked PC seasonality across all four sites (coefficient of determination R^2 = 0.82 – 0.92; Fig. 1), notably including both water-sufficient sites (Fig. 1, A to C), which increase photosynthesis (i.e., "green-up") in the dry season, and a water-limited site (Fig. 1D), which decreases photosynthesis in the dry season. PC phenology thus appears to be the primary driver of GEP seasonality in these forests. This contrasts with most ecosystem models, which represent tropical evergreen forests' GEP seasonality as arising primarily from climate variability interacting with aseasonal photosynthetic infrastructure (*8*, *10*). It also contrasts with observations at shorter diel time scales, during which large GEP changes closely track light levels (photosynthetically active radiation, PAR), whereas PC remains fixed (fig. S11).

We then evaluated the second question: What are the mechanisms driving seasonal changes in PC? We first used tower-mounted cameras—widely used in temperate zones (*16*), but not previously in the tropics (*15*)—to observe dynamics of leaf quantity metrics in three forests (the drier k67 site near Santarém, the wetter k34 site near Manaus, and ATTO in between Santarém and Manaus; fig. S1).

We found that seasonality in camera-derived leaf area index (LAI) (*15*) (figs. S5 and S8) and in the fraction of PAR absorbed by leaves (FAPAR)—

common biotic drivers in photosynthesis models—were insufficient to account for PC seasonality at the two sites with long-term eddy flux measurements (Fig. 2, A to D). Though LAI and FAPAR significantly increased during dry seasons at both sites, their increases preceded PC by at least 1 month, and their relative amplitudes were much smaller than that of PC, which increased proportionally twice as much as LAI and 10 times more than FAPAR. Thus, typical photosynthesis models, which predict that changes in GEP are driven by proportional changes either in PAR (climate) or in FAPAR (biology), would not be able to represent observed photosynthetic seasonality of these forests.

In addition, remotely sensed vegetation activity—as observed by the Enhanced Vegetation Index from Moderate-Resolution Imaging Spectroradiometer (MODIS) [MAIAC EVI, rigorously corrected for clouds, aerosols, and Sun-angle artifacts (*17*)]—closely tracked the magnitude and timing of LAI seasonality (Fig. 2, A to D). In sum, though phenological metrics of leaf quantity from multiple platforms (ground, tower, and satellite) all showed consistent dry-season increases in the central Amazon, these increases were systematically too small to explain the variation in PC that we found is responsible for GEP dynamics in these forests (Fig. 2, C and D).

Next, investigating effects of leaf quality (photosynthetic capacity per leaf area) (*9*, *11*, *18*), we found that increasing leaf losses (litterfall) during dry seasons are more than compensated by simultaneous increases in new leaf production (Fig. 2, E and F). This dynamic drives net increases in
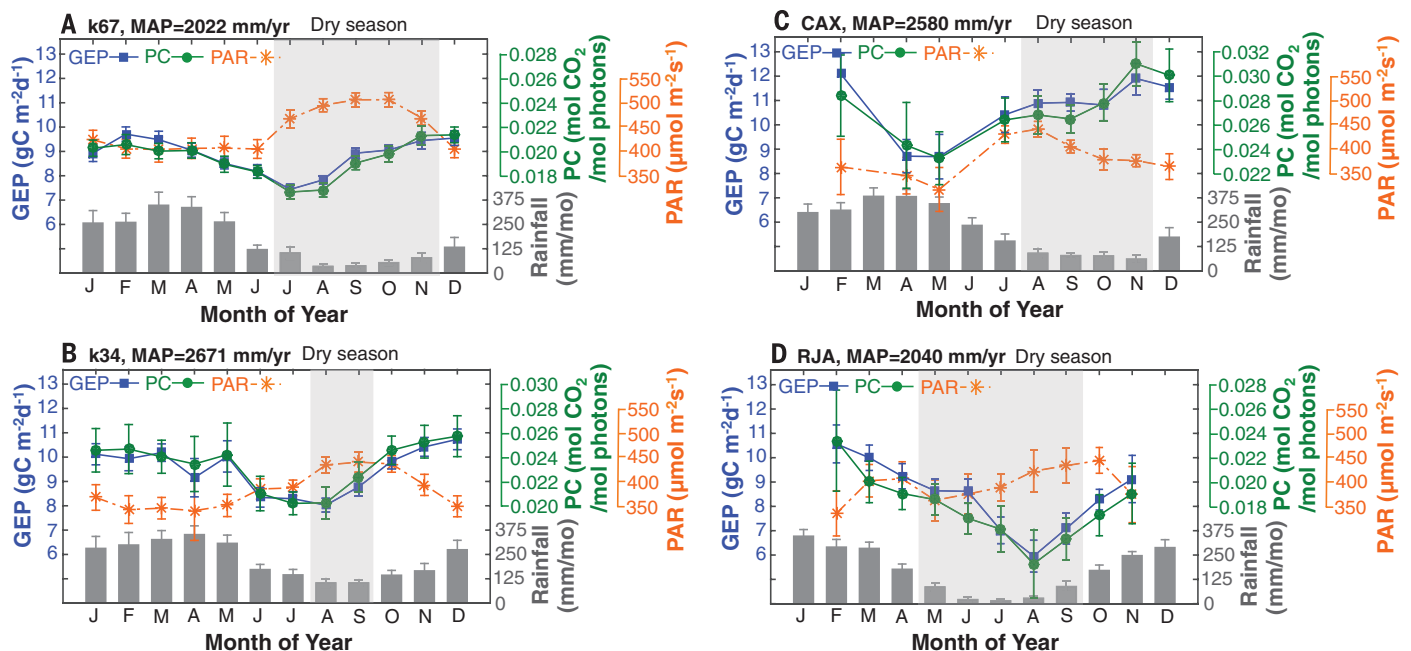

Fig. 1. Gross ecosystem productivity (GEP) seasonality at four Amazon forests is highly correlated with seasonality in intrinsic canopy photosynthetic capacity (PC), but not with seasonality in climatic driving variables (rainfall and photosynthetically active radiation, PAR). Flux tower sites are in three equatorial forests: (**A**) Tapajós National Forest (k67 site near Santarém); (**B**) Cuieiras Reserve (k34 site near Manaus); (**C**) Caxiuana National Forest (CAX near Belem); and in one southern (10°S) forest, (**D**) the Jaru Reserve (RJA) (*15*). Monthly values of GEP, PC, and PAR are averages from 2002–2005 and 2009–2011 at k67 (*n* = 7 years), 1999–2006 at k34 (*n* = 8), 1999–2003 at CAX (*n* = 4), and 1999–2002 at RJA (*n* = 3). Error bars are ± 1 SEM. MAP, mean annual precipitation. Shading indicates dry seasons.

LAI, but also significantly shifts the age composition of these canopies toward younger leaves, which should have higher average "quality" than the older leaves they replace (*11*, *19*).

To test whether simultaneous changes in leaf quantity and quality could account for the large variations in PC and thus GEP, we represented their dynamics in a "leaf demography-ontogeny model" (*15*) (fig. S10). In this model, demography partitions leaf quantity (LAI) into separate age classes, and ontogeny (leaf development) assigns a different "leaf quality" (photosynthetic capacity) to each age class, and these jointly determine ecosystem PC. Driven by new leaf production (assumed to contribute only to young LAI) and by ground-observed litterfall (assumed to come only from old LAI), and constrained to match the mean seasonality of camera-

observed total LAI, the model is fit by adjusting parameters of leaf aging and leaf quality (*15*) (fig. S10) to optimize the match between simulated and observed PC at the k67 site (Fig. 3A).

Optimized PC simulations closely tracked observed PC at k67 (R^2 = 0.91; Fig. 3A, upper panel), which rose and fell with the simulated abundance of the mature (3 to 5 months old) age class (Fig. 3A, lower panel). This correspondence indicates that the mature leaves have the highest photosynthetic capacity and explains the time lag between PC and total LAI (Fig. 2, A and B) as a consequence of leaf maturation time [the time to transition from young (LAI_Y) to mature (LAI_M), fig. S10]. A sensitivity analysis showed that varying leaf quality alone could explain about twice as much seasonal variation in ecosystem PC as leaf quantity alone, consistent with

a previous simpler analysis at a single site near k67 (*11*). The same leaf demography-ontogeny model [using the same parameters fit for k67, but driven by local k34 LAI and litterfall and scaled so that their mean values match (*15*)] well predicted seasonality of ecosystem PC (R^2 = 0.89; Fig. 3B, upper panel) at k34 near Manaus, 600 km away, with a shorter dry season and more rainfall. That it does this without reparameterization strongly supports leaf demography and ontogeny as general mechanisms of photosynthetic seasonality in central Amazonian forests.

For validation, we found that simulated seasonality of young leaves matches ground-based observations of leaf flushing rates (*12*) (Fig. 4A, R^2 = 0.95) and that differences with age among model-fitted leaf-level photosynthetic parameters were consistent with field-measured maximum
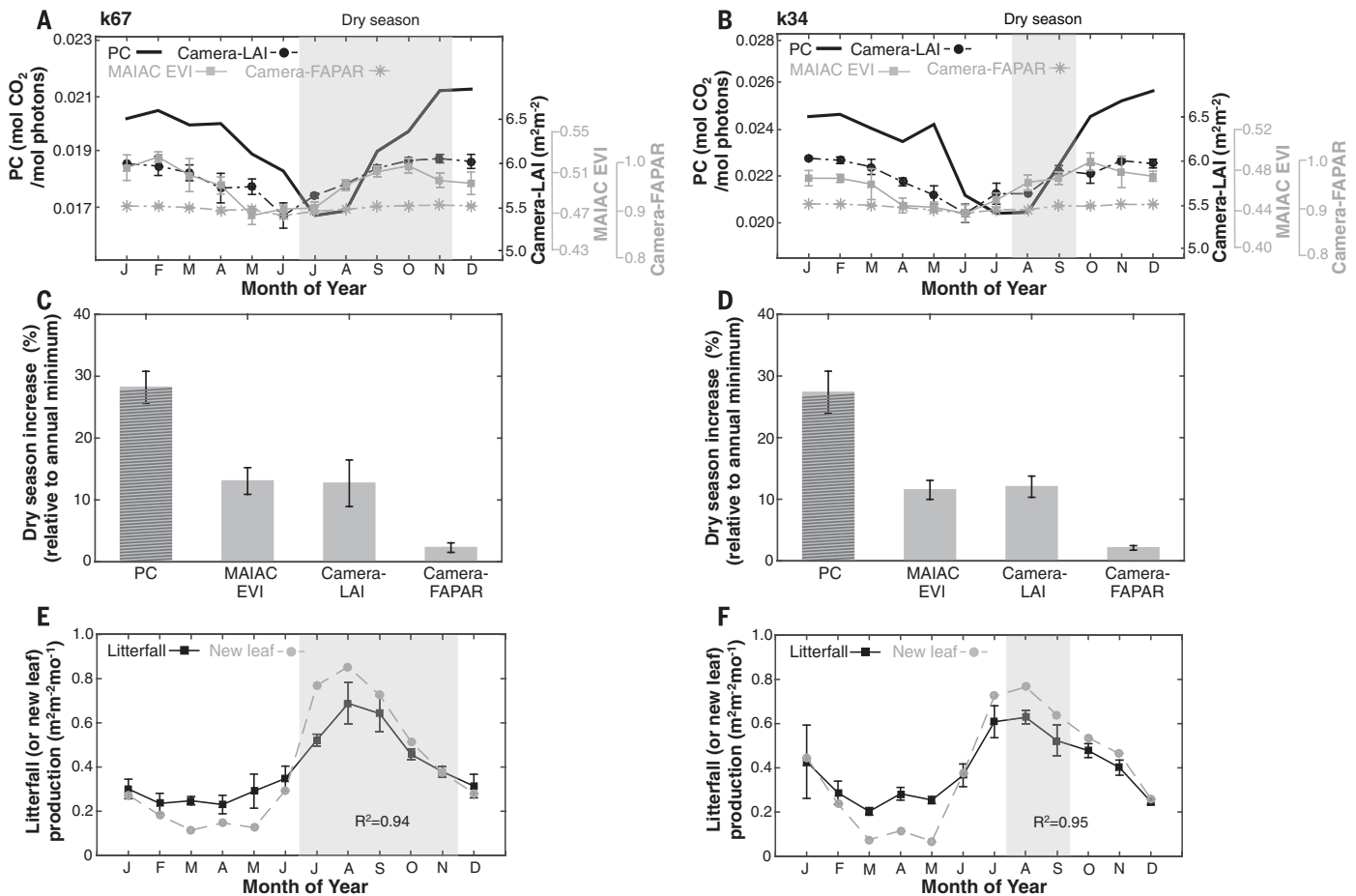

Fig. 2. Leaf quantity alone cannot explain PC seasonality, highlighting the importance of leaf quality. (**A** and **B**) Average annual cycle of photosynthetic capacity (PC) (thick black lines, from Fig. 1) has higher amplitude [at both (A) k67, a long dry-season forest near Santarem, and (B) k34, a short dry-season forest near Manaus] than three key phenological metrics used to drive photosynthesis models: leaf area index (LAI, black circles), fractional absorption of incoming sunlight (FAPAR, gray stars), and the satellite-derived enhanced vegetation index (MAIAC EVI, gray squares). Metrics are scaled so that a given fractional increase is the same magnitude across metrics, relative to the annual minimum. (**C** and **D**) Average dry-season increase (relative to annual minimum) in eddy flux–derived PC (in hatched bars) and its candidate explanatory variables (in gray bars)—satellite-derived MAIAC EVI, camera-

derived LAI, and FAPAR at (C) k67 and (D) k34. (**E** and **F**) Average annual cycle of litterfall (black squares) and new leaf production (gray circles) at the same two sites [(E) k67 and (F) k34] shows that modest dry-season increases in LAI [in (A) and (B)] are associated with rapid leaf turnover due to coordinated leaf loss and new leaf production. Grayed months are local dry season (<100 mm of monthly precipitation). Observations from k67 tower (flux-derived data, 2002–2005 and 2009–2011, n = 7; camera-derived data 2010–2011, n = 2), from a nearby biometric plot (*12*) (litterfall, 2001–2005, n = 5), and from MODIS satellite (2003–2012, n = 10); observations from k34 tower (flux-derived data, 1999–2006, n = 8; camera-derived data 2012–2013, n = 2), from a nearby biometric plot (litterfall, 2004–2008, n = 5), and from MODIS satellite (2003–2012, n = 10). Error bars are ± 1 SEM. Shading indicates dry seasons.

carboxylation rates (V_{cmax}) across these age classes (Fig. 4B). These results substantially advance previous work (*11*) by showing that a common phenological mechanism operates across the central Amazonian rainfall gradient, and by demonstrating this mechanism with a model that could be used to represent leaf demography in larger ecosystem models.

Our study provides evidence that despite enormous biodiversity (*20*), synchronization of leaf phenology patterns among leaf flushing species and at different sites (hundreds of kilometers distant) is sufficient to drive convergent ecosystem-scale seasonal patterns of forest productivity. Such dynamics are not easily captured by standard phenology metrics (LAI,

FAPAR, or satellite vegetation indices like EVI), but are evidently critical for understanding mechanisms underlying evergreen tropical forest functional dynamics.

This work has two implications for understanding controls on tropical forest photosynthesis. First, it reconciles much-debated discrepancies between different spatial scales of observation.
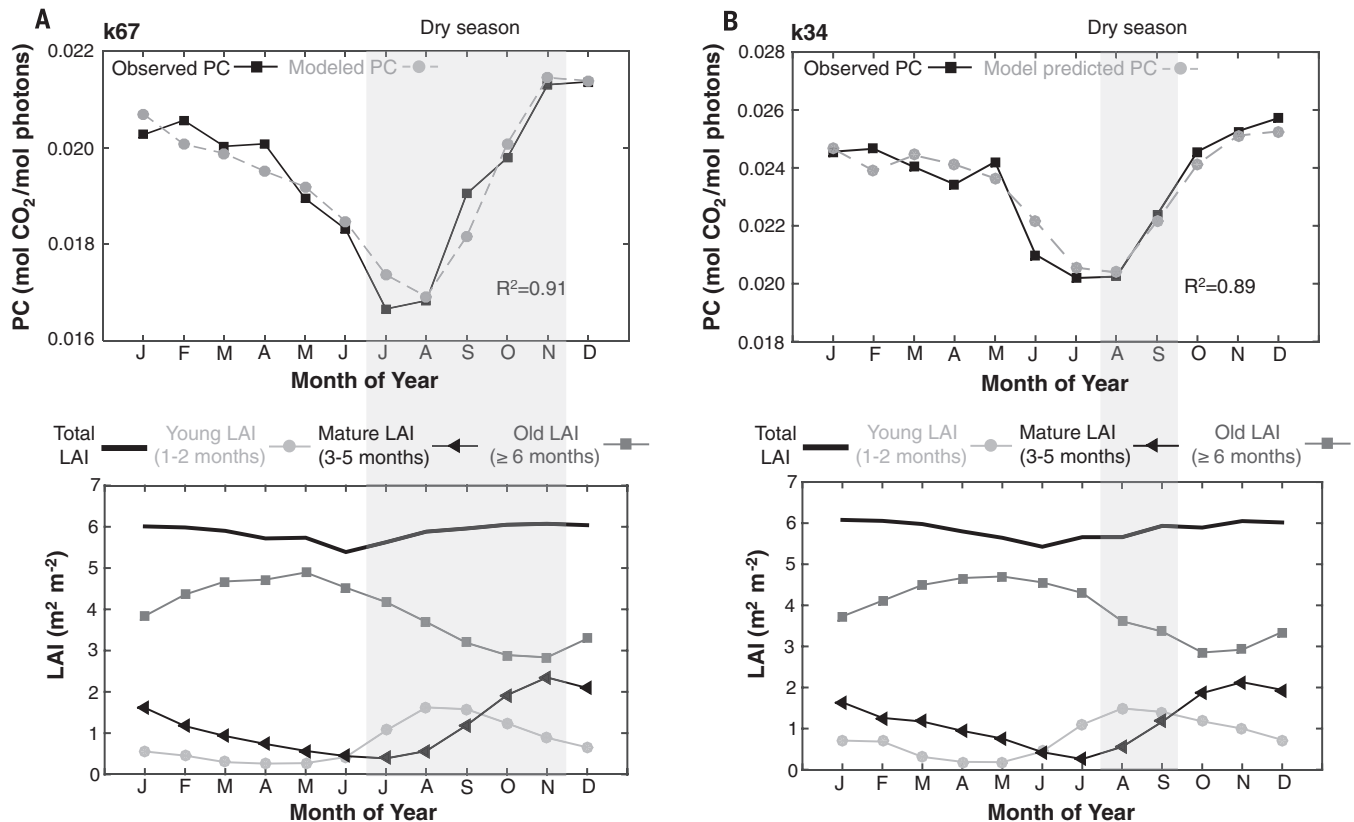
Fig. 3. Leaf demography-ontogeny model simulations. (**A**) Observed and simulated PC seasonality at k67 (upper panel), and associated simulations of LAI in three leaf age classes (three different shades of gray), constrained to sum to total camera-observed LAI (thick black line), with optimal residence times for each age class shown in the legend (lower panel). (**B**) Observed and model-predicted PC seasonality at the wetter k34 site, with parameters optimized for k67 and then scaled to adjust for intersite PC differences (upper panel); associated k34 modeled LAI in three leaf age classes (three different shades of gray); and total camera-observed LAI (black line) (lower panel). Shading indicates dry seasons.
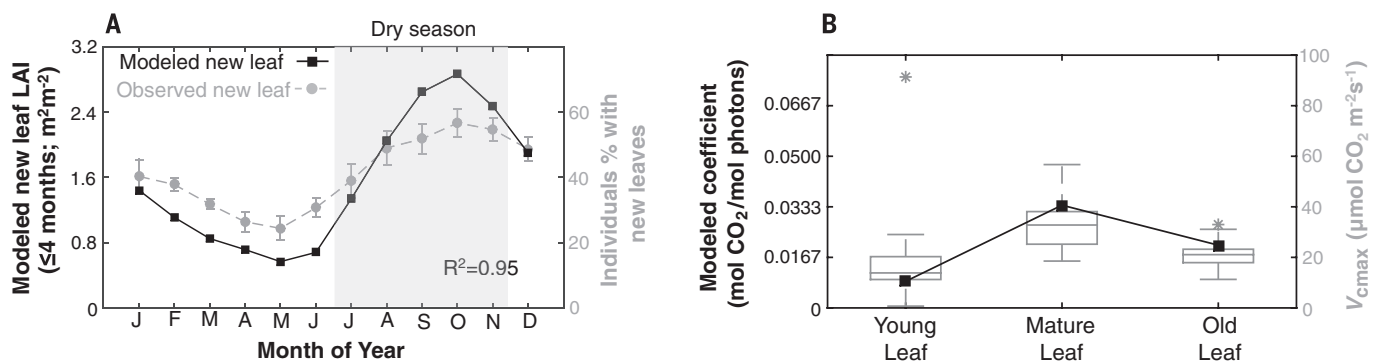

Fig. 4. Validation of leaf demography-ontogeny model. (**A**) Simulations of new leaf age composition (quantity of LAI with age ≤4 months; black squares) along with ground observations of percentage of individuals with new leaves ≤4 months of age (averaged over 1999–2004; *n* = 5) at k67 (gray circles). Shading indicates dry seasons. (**B**) Optimal age-specific photosynthetic efficiency parameters (a_Y, a_M, and a_O; in black squares), compared with age-specific V_{cmax} derived from leaf gas-exchange measurements in 2012 at the k67 site (box plots, in gray, *n* = 5 species × 2 light environments = 10) (*15*). Box plots show median (center line), middle 50% of the distribution (box edges), 1.5 times the interquartile range (whiskers), and outliers (points).

For example, previous work at k67 (*21*) reported little seasonality in leaf-scale photosynthetic parameters, concluding that leaf-level productivity did not explain seasonality of ecosystem productivity. However, that analysis focused on mature leaves only, neglecting the demography and ontogeny here shown to be critical for scaling leaf-level photosynthesis to ecosystems.

At larger scales, this study supports the hypothesis that leaf-demographic mechanisms underlie seasonal increases in tropical vegetation productivity seen from satellites (*6, 7, 13*). And, because leaf stomates link evapotranspiration to photosynthesis, these mechanisms may also facilitate the dry-season maxima in water fluxes (fig. S4). By moistening the dry-season atmospheric boundary layer, these fluxes hasten transition to the wet season ahead of the southward migration of the intertropical convergence zone (*3*). Further, because dry-season water fluxes in South America may influence the timing of the North American Monsoon demise (*22*), tropical leaf phenology may contribute to important ecologically mediated teleconnections (*23*) in the climate system.

The second implication is that leaf phenology is needed to correctly detect, attribute, and model climate sensitivity of tropical forests. Empirical studies that analyze climatic sensitivity of carbon and water fluxes without accounting for phenology (*24, 25*) will misattribute phenological changes to climatic causes. Models that are tuned to match current observations while assuming that LAI or FAPAR are aseasonal risk making erroneous predictions of forest response to future climate changes.

This work highlights the importance of leaf level phenology—especially coordination of leaf growth with senescence—in regulating land surface fluxes of carbon and water, and of associated feedbacks to climate. The causes of phenological patterns may arise from adaptive strategies for avoiding herbivores or pathogens (*26*) or for optimizing plant physiology for carbon gain under seasonal resource availability (*13, 27–29*). Ultimately, understanding the evolutionary and physiological basis for phenological mechanisms may be critical to predicting the long-term response and resiliency of tropical forests to changing climate.

REFERENCES AND NOTES

1. L. Gu et al., in *Phenology: An Integrative Environmental Science*, M.D. Schwartz, Ed. (Kluwer, Netherlands, 2003), pp. 467–485.
2. C. D. Keeling, T. P. Whorf, M. Wahlen, J. van der Plichtt, *Nature* **375**, 666–670 (1995).
3. R. Fu, W. Li, *Theor. Appl. Climatol.* **78**, 97–110 (2004).
4. E. E. Cleland, I. Chuine, A. Menzel, H. A. Mooney, M. D. Schwartz, *Trends Ecol. Evol.* **22**, 357–365 (2007).
5. D. C. Morton et al., *Nature* **506**, 221–224 (2014).
6. J. Bi et al., *Environ. Res. Lett.* **10**, 064014 (2015).
7. A. R. Huete et al., *Geophys. Res. Lett.* **33**, L06405 (2006).
8. I. T. Baker et al., *J. Geophys. Res.* **114**, G00B01 (2008).
9. Y. Kim et al., *Glob. Change Biol.* **18**, 1322–1334 (2012).
10. V. Y. Ivanov et al., *Water Resour. Res.* **48**, W12507 (2012).
11. C. E. Doughty, M. L. Goulden, *J. Geophys. Res.* **113**, G00B06 (2008).
12. P. M. Brando et al., *Proc. Natl. Acad. Sci. U.S.A.* **107**, 14685–14690 (2010).
13. K. Guan et al., *Nat. Geosci.* **8**, 284–289 (2015).
14. B. O. Christoffersen et al., *Agric. For. Meteorol.* **191**, 33–50 (2014).
15. Materials and methods are available as supporting material on *Science* Online.
16. A. D. Richardson, B. H. Braswell, D. Y. Hollinger, J. P. Jenkins, S. V. Ollinger, *Ecol. Appl.* **19**, 1417–1428 (2009).
17. A. I. Lyapustin et al., *Remote Sens. Environ.* **127**, 385–393 (2012).
18. N. Restrepo-Coupe et al., *Agric. For. Meteorol.* **182-183**, 128–144 (2013).
19. K. Kitajima, S. Mulkey, S. Wright, *Am. J. Bot.* **84**, 702–708 (1997).
20. S. Fauset et al., *Nat. Commun.* **6**, 6857 (2015).
21. T. F. Domingues, L. A. Martinelli, J. R. Ehleringer, *Plant Ecol. Divers.* **7**, 189–203 (2014).
22. R. Fu, P. A. Arias, H. Wang, in *The Monsoons and Climate Change*, L.M.V. de Carvalho, C. Jones, Eds. (Springer, 2015), pp. 187–206.
23. S. C. Stark et al., *Landsc. Ecol.* **31**, 181–194 (2016).
24. C. E. Doughty, M. L. Goulden, *J. Geophys. Res.* **114**, G00B07 (2008).
25. J. E. Lee et al., *Proc. Biol. Sci.* **280**, 20130171 (2013).
26. R. Lieberei, *Ann. Bot. (London)* **100**, 1125–1142 (2007).
27. S. Elliott, P. J. Baker, R. Borchert, *Glob. Ecol. Biogeogr.* **15**, 248–257 (2006).
28. S. J. Wright, C. P. van Schaik, *Am. Nat.* **143**, 192–199 (1994).
29. K. Kikuzawa, *Can. J. Bot.* **73**, 158–163 (1995).

CIRCADIAN RHYTHMS

Synchronous *Drosophila* circadian pacemakers display nonsynchronous Ca²⁺ rhythms in vivo

Xitong Liang, Timothy E. Holy, Paul H. Taghert*

In *Drosophila*, molecular clocks control circadian rhythmic behavior through a network of ~150 pacemaker neurons. To explain how the network's neuronal properties encode time, we performed brainwide calcium imaging of groups of pacemaker neurons in vivo for 24 hours. Pacemakers exhibited daily rhythmic changes in intracellular Ca^{2+} that were entrained by environmental cues and timed by molecular clocks. However, these rhythms were not synchronous, as each group exhibited its own phase of activation. Ca^{2+} rhythms displayed by pacemaker groups that were associated with the morning or evening locomotor activities occurred ~4 hours before their respective behaviors. Loss of the receptor for the neuropeptide PDF promoted synchrony of Ca^{2+} waves. Thus, neuropeptide modulation is required to sequentially time outputs from a network of synchronous molecular pacemakers.

Circadian clocks help animals adapt their physiology and behavior to local time. The clocks require a highly conserved set of genes and proteins (*1*) operating through molecular feedback loops to generate robust rhythms that produce a 24-hour timing signal (*2*). These clocks are expressed by pacemaker neurons, which themselves are assembled into an interactive network (*3*). Through network encoding and cellular interactions, pacemaker neurons in the suprachiasmatic nucleus (SCN) of the mammalian brain coordinate many circadian rhythmic outputs (*4–7*). To study how molecular clocks couple to network encoding and how network encoding relates to specific behavioral outputs, we conducted an in vivo brainwide analysis of the circadian

Department of Neuroscience, Washington University School of Medicine, St. Louis, MO 63110, USA.
*Corresponding author. E-mail: taghertp@pcg.wustl.edu

Science

Leaf development and demography explain photosynthetic seasonality in Amazon evergreen forests

Jin Wu, Loren P. Albert, Aline P. Lopes, Natalia Restrepo-Coupe, Matthew Hayek, Kenia T. Wiedemann, Kaiyu Guan, Scott C. Stark, Bradley Christoffersen, Neill Prohaska, Julia V. Tavares, Suelen Marostica, Hideki Kobayashi, Mauricio L. Ferreira, Kleber Silva Campos, Rodrigo da Silva, Paulo M. Brando, Dennis G. Dye, Travis E. Huxman, Alfredo R. Huete, Bruce W. Nelson and Scott R. Saleska

Leaf seasonality in Amazon forests

Models assume that lower precipitation in tropical forests means less plant-available water and less photosynthesis. Direct measurements in the Amazon, however, show that production remains constant or increases in the dry season. To investigate this mismatch, Wu *et al.* use tower-based cameras to detect the phenology (i.e., the seasonal patterns) of leaf dynamics in tropical tree crowns in Amazonia, Brazil, and relate this to patterns of CO_2 flux. Accounting for age-dependent variation among individual leaves and crowns is necessary for understanding the seasonal dynamics of photosynthesis in the entire ecosystem. Leaf phenology regulates seasonality of the carbon flux in tropical forests across a gradient of climate zones.
Science, this issue p. 972

ARTICLE TOOLS	http://science.sciencemag.org/content/351/6276/972
SUPPLEMENTARY MATERIALS	http://science.sciencemag.org/content/suppl/2016/02/24/351.6276.972.DC1
REFERENCES	This article cites 60 articles, 2 of which you can access for free http://science.sciencemag.org/content/351/6276/972#BIBL
PERMISSIONS	http://www.sciencemag.org/help/reprints-and-permissions

Use of this article is subject to the Terms of Service